Colloquium: Modeling the unconventional superconducting properties of expanded A_3C_{60} fullerides

Massimo Capone

SMC, CNR-INFM Dipartimento di Fisica, Università "La Sapienza," P.le Aldo Moro 2, I-00185 Roma, Italy, and ISC-CNR, Via dei Taurini 19, I-00185 Roma, Italy

Michele Fabrizio

International School for Advanced Studies (SISSA), and CNR/INFM DEMOCRITOS National Simulation Center, Via Beirut 2-4, I-34014 Trieste, Italy and The Abdus Salam International Center for Theoretical Physics (ICTP), P.O. Box 586, I-34014 Trieste, Italy

Claudio Castellani

Dipartimento di Fisica, Università "La Sapienza," P.le Aldo Moro 2, I-00185, Roma, Italy

Erio Tosatti

International School for Advanced Studies (SISSA), and CNR/INFM DEMOCRITOS National Simulation Center, Via Beirut 2-4, I-34014 Trieste, Italy and The Abdus Salam International Center for Theoretical Physics (ICTP), P.O. Box 586, I-34014 Trieste, Italy

(Published 19 June 2009)

The trivalent alkali fulleride solids of generic composition A_3C_{60}, where C_{60} is the fullerene molecule and A=K, Rb, and Cs, are a well-established family of molecular superconductors. The superconductive electron pairing is of regular *s*-wave symmetry and is accounted for by conventional coupling of electrons to phonons, in particular by well-understood Jahn-Teller intramolecular C_{60} vibrations. A source of renewed interest in these systems is the surprising indication of strong electron-electron repulsion phenomena, which has emerged in compounds where the C_{60}-C_{60} distance is expanded, by either a large cation size or other chemical or physical means. Several examples are now known where this kind of expansion, while leading to a high superconducting temperature at first, gradually or suddenly causes a decline of superconductivity and its eventual disappearance in favor of a Mott insulating state. This type of insulating state is the hallmark of strong electron correlations in cuprate and organic superconductors, and its appearance suggests that fullerides might also be members of that family. Our approach to fullerides is theoretical, and based on the solution of a Hubbard-type model, where electrons hop between molecular sites. In a Hubbard model of fullerides, unlike models for the strongly correlated cuprates, all important electron correlations occur within the molecular site, so it is efficiently soluble in the dynamical mean-field theory (DMFT) approximation. DMFT solutions confirm that superconductivity in this model fulleride, although of *s*-wave symmetry rather than *d*-wave, shares many of the properties that are characteristic of high-T_c cuprates. The calculations are heavy, and while the working model used is several years old, the new results presented pertain to the interesting case of three electrons per C_{60} molecule, appropriate to A_3C_{60}, and have become possible only recently due to a stronger computational effort. The zero-temperature phase diagram is calculated as a function of the ratio of intramolecular repulsion parameter U to the electron bandwidth W, the increase of U/W representing the main effect of lattice expansion. The phase diagram is close to that of actual materials, with a dome-shaped superconducting order parameter region preceding the Mott transition for increasing cell volume. Unconventional properties of expanded fulleride superconductors predicted by this model include (i) an energy pseudogap in the normal phase; (ii) a gain of electron kinetic energy and of conducting Drude weight at the onset of superconductivity, as in high-T_c cuprates; (iii) a spin susceptibility and a specific-heat behavior that are not drastically different from those of a regular phonon superconductor, despite strong correlations; and (iv) the emergence of more than one energy scale governing the renormalized single-particle dispersion, electronic entropy, and specific-heat jump. These predictions, which if confirmed should establish fullerides as members of the wider family of strongly correlated superconductors, are discussed in light of existing and foreseeable experiments.

DOI: 10.1103/RevModPhys.81.943 PACS number(s): 71.30.+h, 71.10.Pm, 71.10.Fd

CONTENTS

I. INTRODUCTION

Superconductivity, discovered by Kamerlingh Onnes nearly a century ago (Onnes, 1911) and first explained microscopically back in 1957 in terms of electron pairing by Bardeen, Cooper, and Schrieffer (BCS) (Bardeen *et al.*, 1957a, 1957b) is still a surprisingly lively topic. On the one hand, superconductivity is being constantly discovered in an ever-increasing variety of solid-state compounds. On the other hand, it appears more and more difficult to use basically the same standard theory, essentially BCS theory and its extensions (e.g., see, Parks, 1969) to account for all of them. In this standard conventional theory, superconductivity arises from the condensation of electron pairs, the two electrons usually bound in a pair state of *s*-wave symmetry and held together by exchange of lattice phonons. The Coulomb repulsion between the two electrons opposes pair formation, but it does not suppress superconductivity because screening makes it sufficiently weak.

The surprisingly favorable effect of repulsive electron correlations on superconductivity found in some systems, particularly in high-T_c superconducting cuprates, where electron-electron repulsion is dominant, remains unresolved. An immense amount of experimental and theoretical work has accumulated over the past two decades in the attempt to understand these phenomena; see, e.g., Bennemann and Ketterson (2008). Actually, cuprates are the most spectacular members of a wider class of strongly correlated superconductors including heavy-fermion and organic molecular compounds (Bennemann and Ketterson, 2008), systems for which there is no truly comprehensive theory either. Among other factors, theoretical efforts have been hampered by the general *intersite* nature of electron interactions and correlations in many of these systems, a fact that poses great technical difficulties. In this light, identification of a superconductor family in which correlations are at the same time strong, simple, and *on site* is welcome.

A more crucial element is one of perspective. It has been a widespread prejudice to distinguish between those superconductors for which (as in BCS theory) pairing of electrons takes place in the *s*-wave channel and is mediated by phonons and those for which the mechanism may be electronic and not phononic, and where pairing instead takes place in the *d*-wave channel. Whereas it is widely held that strong repulsive correlations are essential to superconductivity in the latter (Anderson, 1987), they are not considered crucial in the former. The conventional BCS scenario and its extensions, namely, the Migdal-Eliashberg theory (Migdal, 1958; Eliashberg, 1960a, 1960b; Parks, 1969)—a controlled approximation valid when the typical phonon frequency is much smaller than the Fermi energy—are more or less automatically accepted, and used to account for the superconducting properties. In this theory, electron-electron repulsion renormalizes the electron—phonon parameters, lowering the critical temperature T_c rather than enhancing it.

The trivalent alkali-metal fulleride superconductors, reviewed by Ramirez (1994) and Gunnarsson (1997, 2004), are among the systems in which this conventional logic seemingly applies. Fullerides are solid-state compounds of generic composition A_3C_{60}, where C_{60} is the fullerene molecule (Gunnarsson, 2004) and A=K, Rb, and Cs are alkali-metal cations. The three alkalis metals donate a total of $n=3$ electrons to each fullerene, half filling its threefold-degenerate t_{1u} molecular level. Electron hopping between first-neighboring fullerenes gives rise to a metal, where conduction is restricted to the three narrow t_{1u}-derived bands, with a total energy bandwidth of no more than 0.6 eV (Satpathy *et al.*, 1992; Erwin, 1993). Metallic fullerides are generally superconducting, with critical temperatures T_c reaching $\sim$40 K, depending on various factors. An empirically important factor appears to be the cell volume. When the fulleride lattice is chemically expanded, by increasing cation size, insertion of neutral molecules, or else physically expanded by removing pressure, T_c undergoes a definite and systematic change. It rises initially with a good correlation with the C_{60}-C_{60} distance (Yildirim *et al.*, 1995; Gunnarsson, 1997). Further expansion, however, causes T_c to drop, coming eventually through a first-order transition to an insulating state, as discussed later.

A wealth of evidence indicates that superconducting pairing in fullerides is phononic and that the relevant phonons are the stiff intramolecular H_g vibrations of the C_{60} molecule, Jahn-Teller coupled to the t_{1u} conduction electrons (Gunnarsson, 1997). Further support for the apparently BCS nature of superconductivity in fullerides comes from specific-heat jumps that scale linearly with T_c, in agreement with BCS theory (Kortan *et al.*, 1992; Ramirez, 1994; Burkhart and Meingast, 1996), as well as a regular (i.e., not exceedingly high) normal-phase magnetic susceptibility (Kortan *et al.*, 1992; Robert *et al.*, 1998). Superconducting energy gaps are less clearly defined (Gunnarsson, 1997); the gap ratio $2\Delta/T_c \simeq 3.4–4.2$ in K_3C_{60} and Rb_3C_{60} (Ramirez, 1994; Gunnarsson, 1997), but are not far from the BCS value of 3.53. These elements suggest viewing the A_3C_{60} compounds as weakly correlated Fermi-liquid conductors (Ramirez, 1994), though with unusually narrow electron bands, with a large effective mass roughly three free-electron masses (Robert *et al.*, 1998). Even the observed decrease of T_c under applied pressure in K_3C_{60} and Rb_3C_{60} is in qualitative agreement with an increasing bandwidth and decreasing density of states at the Fermi level, which further supports a standard BCS picture.

These reassuring, conventional-looking facts are, however, contrasted by a number of conflicting elements that

are strong enough to cast serious doubts on the general applicability of the BCS scenario to superconductors in this family. These elements are especially apparent in the more expanded fullerides including $(NH_3)_xNaK_2C_{60}$ (Riccó *et al.*, 2003) and Li_3C_{60} (Durand *et al.*, 2003), and in the alloys $Cs_{3-x}K_xC_{60}$ and $Cs_{3-x}Rb_xC_{60}$ (Dahlke *et al.*, 2000). For these expanded compounds T_c decreases upon expansion, in contrast to BCS theory. The electron density of states extracted from the NMR Knight shift is at the same time an increasing function of the lattice parameter, smoothly connecting with that of the unalloyed compounds under pressure (Dahlke *et al.*, 2000). Within BCS theory, that increase should lead to a rise of T_c and not a drop, as observed. The same unconventional behavior is observed in Cs_3C_{60}, the fulleride compound with the highest $T_c \sim 40$ K attained under pressure (Palstra *et al.*, 1995). A novel $A15$ superconducting phase of Cs_3C_{60} with expanded structure has recently been synthesized (Ganin *et al.*, 2008), corresponding to a body-centered-cubic arrangement of fullerenes. Superconductivity emerges under pressure through a first-order nonstructural transition at 4 kbar. The critical temperature T_c first increases with pressure, reaching a dome-shaped maximum of 38 K around 7 kbar, above which T_c drops. Since no structural changes are observed under pressure, the appearance of superconductivity as well as the dome-shaped T_c versus pressure behavior must be ascribed solely to the volume contraction (Ganin *et al.*, 2008). This nonmonotonic behavior of T_c with pressure finds no apparent explanation within the conventional theory.

The basic and striking anomaly of expanded fullerides occurs in compounds with the largest intermolecule distances. In these materials, a relatively modest additional lattice expansion (and minor change of symmetry due to intercalated ammonia) is enough to turn them dramatically from metallic and superconducting to antiferromagnetic and insulating (Durand *et al.*, 2003; Iwasa and Takenobu, 2003).[1] With temperature, antiferromagnetic order in the ammoniated compound $NH_3K_3C_{60}$ (see Fig. 1) changes to paramagnetic disorder at a Néel temperature slightly above ~40 K (Prassides *et al.*, 1999). Even above the Néel temperature, the microwave conductivity in $NH_3K_3C_{60}$ remains several orders of magnitude below that of K_3C_{60} (Kitano *et al.*, 2002), testifying to the Mott insulator (correlation-driven) nature of the insulating phase. Electrons in a lattice give rise to a Mott insulating state when electron-electron repulsion stops their free propagation and the lattice appears as a collection of molecular ions. Correlations lead to an energy gap in their spectrum, even if their number density per cell is odd instead of even as in regular band insulators (Mott, 1990). The proximity of a Mott insulator phase in fullerides had long been advocated in different contexts

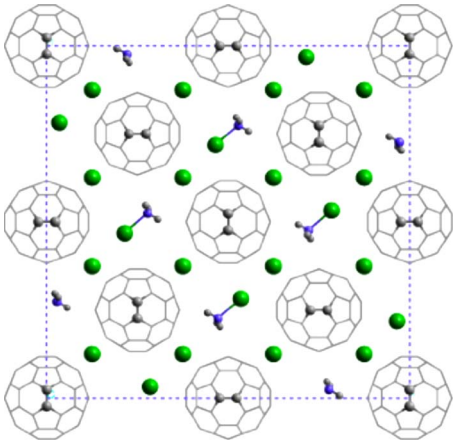

FIG. 1. (Color online) Schematic representation of a planar projection of the crystal structure of $NH_3K_3C_{60}$. Dots are potassium atoms, other dots surrounded by three gray dots are NH_3 molecules, and C_{60} molecules are shown according to their actual spatial orientation. Courtesy of Kosmas Prassides.

(Baskaran and Tosatti, 1991; Chakravarty *et al.*, 1991; Lof *et al.*, 1992; Chakravarty and Kivelson, 2001) but was not taken seriously by the community prior to these data. Superconductivity next to a Mott insulating phase as a function of doping or volume change is the hallmark of strong correlations in high-temperature superconducting cuprates and organics. One is thus naturally led to inquire whether superconductivity in expanded fullerides might, despite the obvious differences, and despite the phononic mechanism, be somehow related to strong correlations. Our contention is that it is indeed closely related, as outlined in the following.

II. ELECTRON INTERACTIONS IN FULLERIDES

The electrons donated by the alkali metals to the C_{60} molecule enter the threefold-degenerate t_{1u} former lowest unoccupied molecular orbital (LUMO). In a degenerate molecular orbital, electrons interact through a variety of mechanisms. The first is overall Coulomb repulsion, which we associate later with the Hubbard parameter U. The second is Coulomb exchange energy, minimized when the molecular state has the highest total spin and the highest total orbital angular momentum compatible with it (Hund's rules) (Landau and Lifshitz, 1958). The third is the Jahn-Teller (JT) interaction, caused by coupling of the electron levels to symmetry-lowering molecular distortions (Landau and Lifshitz, 1958). Contrary to Hund's rules, in a JT-distorted molecule the ground state maximizes double occupancy of levels, thus favoring low total spin instead of high spin in the isolated molecular ion. In molecular C_{60}^{3-}, the strength of these interactions has been evaluated in the past, and the JT strength has been estimated to prevail narrowly over Hund's rule exchange (Lüders *et al.*, 2002) This narrow balance favors a low-spin ground state, with a relatively small "spin gap"—the energy between the low-spin ground state and the lowest high-spin excited

[1]We expect that, below the superconducting pressure of 4 kbar, the new compound $A15$ Cs_3C_{60} (Ganin *et al.*, 2008), yet to be characterized in this respect, should also be an insulating antiferromagnet.

state, expected to be of the order of 0.1 eV (Capone *et al.*, 2001; Lüders *et al.*, 2002). In agreement with this expectation, local moments indicate that, in antiferromagnetic Mott insulating $NH_3K_3C_{60}$, the C_{60}^{3-} sites are in a *low-spin* state, $S=1/2$ (Prassides *et al.*, 1999), their high-spin state $S=3/2$ lying about 100 meV higher in energy. A low spin qualifies the overexpanded fullerides as Mott-Jahn-Teller insulators—that is, Mott insulators whose sites are in a JT-stabilized low-spin state (as opposed to a Hund's rule stabilized high-spin state) (Fabrizio and Tosatti, 1997). Under hydrostatic pressure, $NH_3K_3C_{60}$ undergoes a transition to a metallic state where superconductivity reemerges with a rather large T_c (Prassides *et al.*, 1999). It is important to note that this superconducting phase still belongs to the "expanded" family, as signaled by the fact the T_c here increases further with increasing pressure [reaching 28 K at 14.8 kbar (Zhou *et al.*, 1995)] at variance with nonexpanded fullerides, where T_c drops under pressure.

A lateral but relevant additional element comes from *tetravalent* compounds A_4C_{60}, which are insulators or near insulators. By comparison with the trivalent fullerides, the slight reduction of band-energy gain per particle caused by adding one more electron per molecule and by slightly changing the crystal structure is sufficient to turn the trivalent metals into tetravalent insulators even in nonexpanded materials. Careful density-functional electronic-structure calculations indicated that it is not possible to describe the tetravalent compounds such as K_4C_{60} as statically distorted Jahn-Teller band insulators (Capone *et al.*, 2000). A static JT distortion and the associated orthorhombic state is actually present only in Cs_4C_{60} (Dahlke and Rosseinsky, 2002), and in Rb_4C_{60} above a critical pressure (Huq and Stephens, 2006), while it never shows up in K_4C_{60} (Huq and Stephens, 2006) [with the exception of monolayers; see Wachowiak *et al.* (2005)]. The persistence of insulating or near-insulating behavior and the recovery of molecular symmetry observed in the high-temperature phase of tetravalent fullerides suggests that these compounds too are Mott-Jahn-Teller insulators (Knupfer and Fink, 1997; Capone *et al.*, 2000; Klupp *et al.*, 2006), like the overexpanded trivalent materials. The dynamic JT effect in each C_{60}^{4-} ion associated with Mott localization of carriers is crucial in explaining the low-spin ground state and the spin gap of A_4C_{60}, exactly as for the expanded trivalent compounds.

From the above discussion, one might be tempted to conclude that strong correlations play a role only in tetravalent and expanded trivalent compounds, while face-centered-cubic (fcc) K_3C_{60} and Rb_3C_{60}, where superconductivity was originally discovered, could still be viewed as weakly correlated systems, and as BCS-type superconductors. We do not believe in this conclusion. A final, independent, and strongly unconventional signal is provided by NMR. In fact, NMR data show direct evidence of a spin gap of order 0.1 eV, appearing as an anomalous activated increase of inverse relaxation time. Most likely this gap between a low-spin ground state and a high-spin excited state reflects the multiplet behavior of the localized C_{60}^{n-} molecular ion. It shows up ubiquitously in all alkali-metal-doped fullerides, including superconducting fcc compounds (Thier *et al.*, 1995; Brouet *et al.*, 2002a, 2002b). The existence of the spin gap signifies that the magnetic response of fullerides is very far from Fermi-liquid behavior, which has no such feature. Magnetically the fullerides behave as if localized molecular multiplet excitations coexisted with delocalized propagating quasiparticles. As discussed, the recovery of molecular physics is characteristic of Mott insulators, suggesting that the fingerprint of Mott physics is strongly present already in the nonexpanded superconducting fcc compounds. This suggests that the fcc compounds are somehow the analogs of the overdoped cuprates, whereas the expanded trivalent materials are analogous to the underdoped cuprates. The conclusion is that both are crucially, even if differently, influenced by electron correlations.

We believe that the above elements are strong enough to call for a new physical picture for the whole family of A_3C_{60} superconductors. The proximity of the Mott insulator strongly suggests that the anomalies of expanded fullerene superconductors most likely originate from strong repulsive electron correlation in the narrow t_{1u} bands. The prevalence in the Mott-localized state of molecular physics, with its orbital degeneracy, JT effect, and intramolecular exchange, must be taken into account along with itinerant-electron band physics. Upon expanding the cell volume, the intermolecular hopping of electrons weakens, whereas all the on-site correlation terms—Coulomb and exchange electron-electron interactions as well as the molecular JT effect—are likely to become increasingly relevant. We are led to a picture in which the Mott insulator physics of weakly coupled molecular ions prevails progressively over band physics for increasing lattice expansion. In particular, superconductors that operate in this regime are bound to deviate from the standard Migdal-Eliashberg scenario, the more so as the lattice spacing increases. To investigate that regime, we need to start with a broader theoretical scheme for trivalent fullerides, capable of describing their behavior under lattice expansion and near the Mott transition. While that has been the scope of our past work, previous work was limited for practical technical reasons to tetravalent systems (Capone *et al.*, 2000, 2001, 2002). The study of A_3C_{60} systems, computationally much heavier due to the simultaneous relevance of magnetic and orbital ordering, has only now been completed, and we offer here an outline of the main results.

III. MODEL AND INTERACTIONS

Our theoretical model of trivalent fullerides assumes a lattice of molecular sites, each representing a C_{60} molecule. The C_{60} t_{1u} threefold-degenerate LUMO can for all purposes be treated as an atomic p level. An average of three electrons per molecule are donated by alkali-metal atoms and partially fill these orbitals, which can host up to six electrons. The electrons hop from site to

site, giving rise to half-filled bands of width $W \sim 0.6$ eV. On each site, the electrons experience a Hubbard repulsion $U \sim 1$ eV (corresponding to the Slater integral $F_0 \propto U$),

$$\mathcal{H}_U = (U/2)(n-3)^2, \tag{1}$$

together with a weaker interorbital Hund's rule exchange coupling term J_H, proportional to the Slater integral F_2. Under the sole assumption of full rotational orbital symmetry, this exchange term takes the form (Capone *et al.*, 2001, 2002)

$$\mathcal{H}_J = J(2\mathbf{S}\cdot\mathbf{S} + \tfrac{1}{2}\mathbf{L}\cdot\mathbf{L}) + \tfrac{5}{6}J(n-3)^2, \tag{2}$$

where $J=-J_H<0$, while n, $\mathbf{S}$, and $\mathbf{L}$ are the density, spin, and orbital angular momentum operators, defined as for p orbitals, on the given site. This exchange term favors high $\mathbf{S}$ and $\mathbf{L}$ molecular multiplets, and has been overlooked or neglected in most treatments so far. The next interaction is the JT intramolecular coupling of electrons in the t_{1u} orbital to H_g intramolecular vibrations. This interaction, on the contrary, has been discussed widely [see, e.g., Lannoo *et al.* (1991), Varma *et al.* (1991), Auerbach *et al.* (1994), Gunnarsson *et al.* (1995), and references therein], and we will not dwell too much on its details here. It acts to split the t_{1u} orbital degeneracy and thus favors low-spin states, effectively playing the opposite role to intramolecular exchange. A proper treatment of the JT coupling involves the dynamics of carbon nuclei in C_{60}^{n-} ions, including retardation, and has been developed by Gunnarsson *et al.* (1995). However, for expanded fullerides close enough to the Mott transition, retardation is not essential and can be omitted. In fact, in this regime the intersite motion of quasiparticles is severely slowed down and the coherent bandwidth will eventually drop from W to ZW ($Z \ll 1$). When ZW falls enough to approach the relatively high H_g vibration frequencies of fullerene, $\hbar\omega \sim 90$ meV (Capone *et al.*, 2000, 2001, 2002), quasiparticles begin to move on a comparable time scale with the vibrating carbon atoms, and nonadiabatic effects become important (Cappelluti *et al.*, 2000). Even closer to the Mott transition, the phonon dynamics becomes eventually *faster* than intermolecular quasiparticle hopping. In this antiadiabatic limit, molecular vibrations can be integrated away, and the resulting unretarded effective JT interaction recovers identically the same form as Hund's rule exchange (2) except for the sign of J, namely, $J_{\mathrm{JT}}>0$ (Capone *et al.*, 2001). In this limit, the Hund and JT intramolecular interorbital interaction terms can be directly combined in the form (2) with $J=-J_H+J_{\mathrm{JT}}$. In C_{60}, $J_H \simeq 0.03$–0.1 eV (Martin and Ritchie, 1993; Lüders *et al.*, 2002), whereas $J_{\mathrm{JT}} \simeq 0.06$–$0.12$ eV (Lannoo *et al.*, 1991; Varma *et al.*, 1991; Auerbach *et al.*, 1994; Gunnarsson *et al.*, 1995; Lüders *et al.*, 2002). The total result—and the only one compatible with s-wave superconductivity, a spin-1/2 Mott insulator, and a moderate spin gap near 0.1 eV—is a relatively weak unretarded attraction that has the form of an *inverted* Hund's rule coupling (Capone *et al.*, 2002; Granath and Östlund, 2003). This is the approximation we adopt, keeping in mind that it is strictly valid only when $ZW<\hbar\omega$, that is, close enough to the Mott transition.

The lattice expansion characterizing the expanded fullerides is believed to have little effect on either J_H or J_{JT}. On the other hand, expansion will surely decrease W and increase U, so it can be modeled as a gradual increase of U/W, reflecting both the band narrowing due to smaller overlap between molecular wave functions and a decreased screening strength. As discussed above, this Hamiltonian model, even if not really simple, has many-body interactions that are strictly on site, an ideal situation for dynamical mean-field theory (DMFT) (Georges *et al.*, 1996), one popular and powerful tool in the field of strongly correlated electron systems; we describe it in the next section.

A. Dynamical mean-field theory

DMFT is a quantum version of classical mean-field theory, which provides an exact description of the local dynamics, at the price of freezing away all spatial fluctuations. The mean-field scheme is formulated by a mapping of the lattice model onto an Anderson impurity model (AIM) embedded in a free-electron Fermi "bath" subject to a self-consistency condition (Georges *et al.*, 1996). In our model, the effective AIM is threefold orbitally degenerate, with p-like levels representing the t_{1u} orbitals, each hybridized with a bath. The Hamiltonian is

$$\mathcal{H} = \mathcal{H}_U + \mathcal{H}_J + \sum_{ka\sigma} \varepsilon_{ka} c^\dagger_{ka\sigma} c_{ka\sigma} + \sum_{ka\sigma} V_{ka}(c^\dagger_{ka\sigma} p_{a\sigma} + \mathrm{H.c.}), \tag{3}$$

where $\mathcal{H}_U$ and $\mathcal{H}_J$ are Eqs. (1) and (2) for fermions on the impurity orbitals, ε_{ka} are the bath energy levels labeled by the index k and an orbital index $a=x, y, z$, and V_{ka} are the hybridization parameters between the bath fermions, created by $c^\dagger_{ka\sigma}$, and the impurity fermions, created by $p^\dagger_{a\sigma}$. The mean-field scheme implies a self-consistency condition that depends on the impurity Green's function and on the bare density of states of the original lattice. Throughout our calculations, we use an infinite-coordination Bethe lattice, whose density of states is semicircular. This is a reasonable description of a realistic three-dimensional density of states devoid of accidental features such as van Hove singularities. It is, moreover, particularly convenient since it leads to a very simple and transparent form of the self-consistency condition. The Bethe lattice is the $z\to\infty$ limit of a Cayley tree of coordination z, scaling the nearest-neighbor hopping in each of the z directions as $t/\sqrt{z}$. The resulting semicircular density of states has a bandwidth of $4t$.

The self-consistency condition requires the so-called Weiss field (i.e., the noninteracting Green's function of the AIM),

$$\mathcal{G}_0^{-1}(i\omega_n)_a = (i\omega_n + \mu) - \sum_k \frac{V_{ka}^2}{i\omega_n - \varepsilon_{ka}}, \tag{4}$$

to be related to the local interacting Green's function $G_a(i\omega_n)$ not only through the Dyson equation for the AIM,

$$\mathcal{G}_0^{-1}(i\omega_n)_a = G_a^{-1}(i\omega_n) + \Sigma_a(i\omega_n),$$

which requires the full solution of the impurity model, but also by the additional self-consistency equation

$$\mathcal{G}_{0a}^{-1}(i\omega_n) = (i\omega_n + \mu) - t^2 G(i\omega_n)_a. \tag{5}$$

DMFT for a given model thus amounts to solving the AIM iteratively until the impurity Green's function satisfies Eq. (5). In this work, we solved the threefold-degenerate AIM by exact diagonalization. That requires truncating the sum over k in Eqs. (3) and (5) to a finite and relatively small number of baths N_b, so that the Hamiltonian can be diagonalized in the finite resulting Hilbert space. We generally used $N_b=4$ for each orbital. Most of the results we present are at zero temperature, where we can use the Lanczos algorithm to calculate the Green's function without fully diagonalizing the Hamiltonian. The finite-temperature results for the specific heat and its jump at T_c reported in Sec. V are the exception. They are obtained by means of the finite-temperature extension of Lanczos (Capone *et al.*, 2007), where the thermal Green's function is expressed as a sum over the low-lying eigenvectors $|n\rangle$ and eigenvalues E_n of the impurity model,

$$G_{a\sigma}(i\omega_n) = \frac{1}{Z}\sum_m e^{-\beta E_m} G_{a\sigma}^{(m)}(i\omega_n), \tag{6}$$

with

$$G_{a\sigma}^{(m)}(i\omega_n) \equiv \sum_n \frac{|\langle n|p_{a\sigma}|m\rangle|^2}{E_m - E_n - i\omega_n} + \sum_n \frac{|\langle n|p_{a\sigma}^\dagger|m\rangle|^2}{E_n - E_m - i\omega_n}. \tag{7}$$

The Boltzmann factor in Eq. (6) guarantees that the lower the temperature, the smaller the number of excited states that actually contribute to the Green's function. Therefore, for sufficiently low temperature, we can still use the Lanczos algorithm to find the lowest-energy eigenstates. In practice, only a limited number of states, 20–25, can be calculated in a reasonable time. Unfortunately, this number is insufficient to make the truncation error in Eq. (6) negligible for the present model in the relevant correlated regime. We estimate the systematic error on the Green's function to be of order of a few percent, a level of accuracy that does not allow us to determine fully such thermodynamic properties as the critical temperature. Luckily, this error affects the absolute specific-heat value much more than its relative changes, including the superconducting jump in units of T_c, discussed further below (see Sec. V). We underline that this limitation does not affect by any means the $T=0$ calculations.

The above DMFT equations refer to a paramagnetic phase in which no symmetry breaking occurs. However, in this work we are interested in s-wave superconducting and in antiferromagnetic solutions, where symmetry is broken. Superconductivity is conveniently studied in the Nambu-Gor'kov representation by introducing spinors

$$\psi_{\mathbf{k}a} = \begin{pmatrix} p_{\mathbf{k}a\uparrow} \\ p_{-\mathbf{k}a\downarrow}^\dagger \end{pmatrix},$$

and defining accordingly the Green's function $G_{\mathbf{k}a}(\tau) = -\langle T_\tau[\psi_{\mathbf{k}a}(\tau)\psi_{\mathbf{k}a}^\dagger(0)]\rangle$ in imaginary time as a 2×2 matrix that satisfies the Dyson equation in Matsubara frequencies,

$$G_{\mathbf{k}a}(i\omega) = G_{\mathbf{k}a}^0(i\omega) + G_{\mathbf{k}a}^0(i\omega)\Sigma(i\omega)G_{\mathbf{k}a}(i\omega), \tag{8}$$

with $G_{\mathbf{k}a}^0(i\omega)$ the noninteracting value. The single-particle self-energy $\Sigma(i\omega)$ is also a 2×2 matrix whose off-diagonal element $\Delta(i\omega)$, when finite, signals a superconducting phase. The DMFT self-consistency can be written now as

$$\mathcal{G}_0^{-1}(i\omega_n) = i\omega_n\tau_0 + \mu\tau_3 - t^2\tau_3 G(i\omega_n)\tau_3, \tag{9}$$

where τ_0 and τ_3 are Pauli matrices.

Analogously, antiferromagnetism in a bipartite lattice is conveniently described using the spinor

$$\psi_{\mathbf{k}a\sigma} = \begin{pmatrix} p_{\mathbf{k}a\sigma} \\ p_{\mathbf{k}+\mathbf{Q}a\sigma} \end{pmatrix},$$

with $\mathbf{k}$ in the magnetic Brillouin zone and $\mathbf{Q}$ the modulation vector. This leads once more to a 2×2 Green's function and self-energy matrices related by the Dyson equation (8). Here too, a finite off-diagonal element signals an antiferromagnetically ordered phase. The self-consistency equation for antiferromagnetism exploits the bipartite property of the lattice. Indicating one sublattice by A and the other by B, the general self-consistency condition is

$$\mathcal{G}_0^{-1}(i\omega_n)_{\sigma A} = (i\omega_n + \mu) - t^2 G(i\omega_n)_{\sigma B}, \tag{10}$$

which becomes Eq. (5) if $G_{\sigma A} \equiv G_{\sigma B}$, i.e., if the system is nonmagnetic. When the system is antiferromagnetic, then $G_{\sigma A} \equiv G_{-\sigma B}$. Thus we can eliminate the sublattice B from Eq. (10), and obtain the following result for the self-consistency equation:

$$\mathcal{G}_0^{-1}(i\omega_n)_{\sigma A} = (i\omega_n + \mu) - t^2 G(i\omega_n)_{-\sigma A}. \tag{11}$$

This equation is valid for a Bethe lattice with nearest-neighbor hopping, a case with perfect nesting that is rather exceptional in realistic antiferromagnets. A way to simulate imperfect nesting typical of more realistic situations, while still taking advantage of the Bethe-lattice simplifications, is to add next-nearest—neighbor hopping t'/z in the Cayley tree (this is merely a device to eliminate nesting, not meant to suggest next-nearest-neighbor hopping, small in fullerides). In the limit $z \to \infty$ of the Bethe lattice, the self-consistency equation becomes

$$\mathcal{G}_0^{-1}(i\omega_n)_{\sigma A} = (i\omega_n + \mu) - t^2 G(i\omega_n)_{\sigma B} - t'^2 G(i\omega_n)_{\sigma A}$$
$$= (i\omega_n + \mu) - t^2 G(i\omega_n)_{-\sigma A} - t'^2 G(i\omega_n)_{\sigma A}. \quad (12)$$

For both broken-symmetry phases, if the diagonal elements of the self-energy matrix at low Matsubara frequencies follow the conventional Fermi-liquid behavior (which we always find to be the case),

$$\Sigma_{\text{diagonal}}(i\omega_n) \simeq (1 - 1/Z) i\omega_n, \quad (13)$$

the actual value of the spectral gap in the single-particle spectrum is given by $Z\Delta(0)$, the zero-frequency anomalous (superconducting or antiferromagnetic) self-energy multiplied by the so-called quasiparticle weight Z.

We conclude by noting that, within DMFT, one can search for solutions with different symmetries by simply allowing or preventing symmetry-breaking order parameters, even in regions where the chosen phase is not the most stable. When two or more solutions coexist, the stable one is determined by an explicit energy calculation. As we discuss, for a wide range of U/W values we do find coexisting superconducting and antiferromagnetic solutions, the former prevailing at smaller U, the latter at larger U. The physical phase diagram thus exhibits a first-order transition between these two symmetry-broken phases—a nonmagnetic s-wave superconductor and an insulating spin-1/2 antiferromagnet—taking place when the respective energy curves intersect.

B. $T=0$ phase diagram

Modeling lattice expansion of fullerides as a gradual increase of U/W, we can proceed to analyze the theoretical zero-temperature "phase diagram" of our model obtained by DMFT as a function of U/W. Starting with the uncorrelated system with $U=0$, the model initially exhibits straight BCS superconductivity driven by JT phonons (i.e., the attractive J we introduced above) with an s-wave ($S=L=0$) order parameter[2]

$$P_{\text{SC}} = \frac{1}{N}\sum_i \sum_{a=x,y,z} \langle p^\dagger_{ia\uparrow} p^\dagger_{ia\downarrow} \rangle, \quad (14)$$

where N is the number of molecules and $p^\dagger_{ia\sigma}$ creates an electron on molecule i, with spin σ and in orbital $a=x,y,z$. The Fermi-liquid scattering amplitude in the Cooper channel, measuring the strength of the effective attraction, is $A=-10J/3$. We note that, owing to fairly strong JT interactions (Auerbach *et al.*, 1994; Gunnarsson *et al.*, 1995), if Hund's exchange J_H were neglected, the dimensionless JT coupling constant of fullerenes controlling superconductivity would be numerically very large, $\lambda = \rho_0 |A| \simeq 0.6$–$1.0$, where ρ_0 ($\simeq 2.4\ \text{eV}^{-1}$) is the bare density of states per spin and orbital. Turning on a weak Coulomb repulsion U on top of that will reduce the pairing attraction in this regime. Perturbatively one obtains for small U that $A=-10J/3+U$. Since J is insensitive to expansion while U/W increases, this implies that in this picture, where Hund's rule exchange is neglected, T_c should always decrease upon expansion, a prediction that is at odds with experiments.

In fact, as anticipated, Hund's rule exchange is not negligible, and its effect is to introduce a substantial cancellation in J, leading to a greatly reduced effective coupling $\lambda_{\text{eff}} \simeq \frac{10}{3}(J_{\text{JT}} - J_H)\rho_0$. Should we interpret the ubiquitous spin gap of 0.1 eV (Thier *et al.*, 1995; Brouet *et al.*, 2002a, 2002b) as the C_{60}^{n-} molecular excitation energy between its low-spin ground state with $S=1/2$ and 0 for $n=3$ and 4, respectively, and its high-spin excited state with $S=3/2$ and 1 for $n=3$ and 4, respectively, we would conclude that, to be consistent with our model where both gaps are equal to $5J$ (Capone *et al.*, 2004), the total effective inverted exchange J, comprehensive of both JT and Hund's rule exchange, should be $J=0.02$ eV. In reality, the qualitative scenario we describe is relatively independent of the precise value of J provided it is inverted, i.e., negative and small.

Once exchange is included, the resulting $\lambda_{\text{eff}} \simeq 0.16$ is now much smaller—in fact, it is much too small to explain within conventional BCS or Migdal—Eliashberg theory any of the observed values of T_c in fullerides [let alone the nonmonotonic behavior of T_c versus the density of states for expanded fullerides (Dahlke *et al.*, 2000; Ganin *et al.*, 2008)]. Things get worse when we increase the on-site Coulomb repulsion U closer to realistic values, $U \sim W$ and beyond. In the conventional weakly correlated picture, U would provide in the electron pairing problem a repulsive Coulomb pseudopotential whose bare value is $\mu_* = U\rho_0 \simeq 3$ (Parks, 1969). Simply comparing these bare values of λ and μ_*, we should conclude that s-wave BCS superconductivity in fullerenes is simply impossible (with the obvious proviso that for small U an unretarded treatment of JT phonon interactions is not really justified).

The full DMFT solution of the model for $J=0.05W$ and increasing U/W yields the phase diagram in Fig. 2. While confirming the above expectations for moderate U, it has a surprise in reserve at larger U values, where the Mott transition is approached.

Figure 3 shows the zero-frequency anomalous single-particle self—energies calculated within DMFT for the superconducting and the antiferromagnetic solutions. At $U=0$, the model is an s-wave BCS superconductor, with an exponentially small superconducting $\Delta(0)$. This is too small to be visible in the figure, since, as mentioned, the effective exchange reduced $\lambda \sim 0.2$ is very weak. Beginning from zero, the increase of U first rapidly destroys the weak BCS superconductivity. The superconducting $\Delta(0)$ vanishes at roughly the mean-field value $U=10/3J$, and above this value of U the ground state becomes a normal metal, as expected. Upon further increase in U/W, the model remains a normal metal—no superconductivity, no antiferromagnetism. However, the impor-

[2]Since gauge symmetry is broken, we are allowed to assume P_{SC} real.

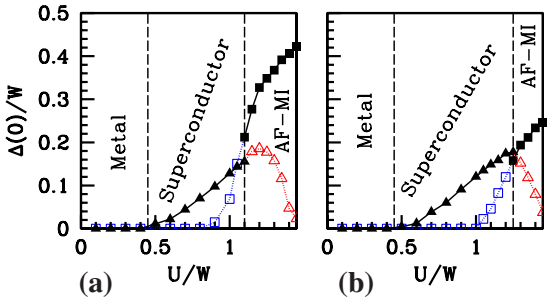

FIG. 2. (Color online) Superconducting solution (triangles) and antiferromagnetic solution (squares) zero-frequency anomalous self-energies $\Delta(0)$ as a function of U/W. Solid symbols are used when the corresponding symmetry-broken phase is stable, while open symbols are used when it is metastable, i.e., has higher energy than the other phase. The first-order transition between the two phases is indicated by a vertical line separating the superconductor from the antiferromagnetic Mott insulator. The case in the presence of a frustrating next-nearest-neighbor hopping $t'=0.3t$, absent in (a).

tance of electron correlations increases with U, as signaled, for example, in the DMFT spectral function (not shown) by the gradual formation of incoherent Hubbard bands on both sides of the Fermi level. The metallic character persists until a hypothetically continuous Mott transition is eventually reached near $U/W\sim1.5$, where $Z=0$ and the metallic character is extinguished.

Before this happens, however, *s*-wave superconductivity reenters from the normal-metal state. The anomalous self-energy $\Delta(0)$, proportional to the superconducting order parameter, has, as a function of U, a bell-shaped behavior—a "superconducting dome" as it is called in cuprates—hitting a large maximum before dropping again. The reentrant superconductive behavior is a clear realization of phonon-induced strongly correlated superconductivity (SCS) (Capone *et al.*, 2002). The sharply rising order-parameter edge with increasing U/W can in our view explain the strong rise of T_c upon lattice expansion in nonexpanded compounds, previously attributed to a BCS-like increase of density of states upon band narrowing. Past the dome maximum, and upon increasing expansion, the SCS superconducting order parameter declines, and would eventually drop to zero at the continuous metal-insulator transition near $U/W\sim1.5$. This continuous decline of superconductivity is preempted by a first-order transition to a lower-energy antiferromagnetic Mott insulating phase, with order parameter

$$P_{\mathrm{AFM}}=(1/N)\sum_i(-1)^i(n_{i\uparrow}-n_{i\downarrow}), \tag{15}$$

where $n_{i\sigma}=\Sigma_{a=x,y,z}p^{\dagger}_{ia\sigma}p_{ia\sigma}$ is the full occupation number with spin σ at molecule i. The exact location of the superconductor-insulator transition depends on details. For strong nesting ($t'=0$), it takes place even before the superconducting dome maximum. In Fig. 3, we show $\Delta(0)$ of Fig. 2 in comparison with the spectral gaps $Z\Delta(0)$, as well as the order parameters P_{SC} and P_{AFM}. Notice that Z for the superconductor is smaller and vanishes at the continuous metal-insulator transition, while Z for the antiferromagnet is of order 1. In both cases, the dimensionless order parameter essentially follows the behavior of the spectral gap.

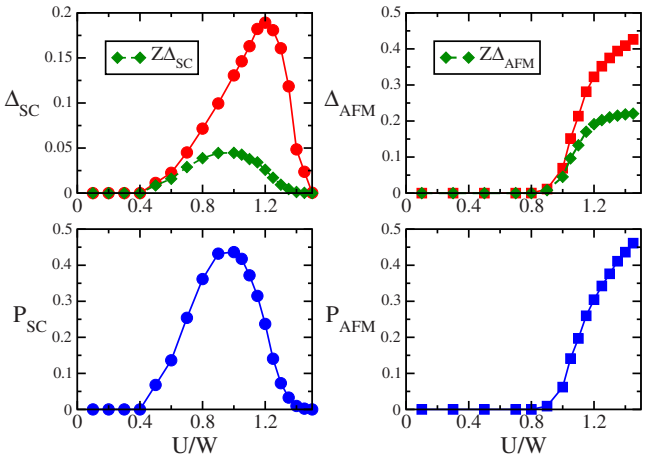

FIG. 3. (Color online) Superconducting solution (SC, left) and antiferromagnetic solution (AFM, right) anomalous self-energies (top) and order parameters (bottom) as functions of U/W. The top panels also show (diamonds) the spectral gaps obtained on multiplying Δ by the quasiparticle weight Z of each solution. The gaps are in units of the bandwidth W (the order parameters are by definition dimensionless).

When we add a next-nearest-neighbor hopping t' to mimic imperfect nesting (which we expect to find generically for realistic band structures, in particular in the face-centered-cubic A_3C_{60} materials), we find that the superconducting phase is only weakly affected but antiferromagnetism is strongly frustrated. As a result, the superconducting region expands at the expense of the magnetic insulator, and the superconducting dome may emerge in full [Fig. 2(b)]. We propose that the gradual drop in the superconducting order parameter past the dome maximum now naturally explains the decline of T_c of expanded fullerides (Dahlke and Rosseinsky, 2002; Durand *et al.*, 2003; Ganin *et al.*, 2008).

Finally, past the first-order Mott transition, we find that the antiferromagnetic insulator is formed mainly by spin-1/2 local configurations, which is in agreement with experiments in $NH_3K_3C_{60}$ (Iwasa and Takenobu, 2003). We also predict that ambient-pressure $A15$ Cs_3C_{60}, yet to be characterized, should similarly be a spin-1/2 antiferromagnetic insulator. Besides spin rotational symmetry, this kind of state also breaks orbital rotational symmetry, signaling that spin ordering must be generally accompanied by orbital ordering. In ammoniated fullerides, that again is consistent with experiment (Iwasa and Takenobu, 2003). We conclude that, in spite of strong simplifying assumptions, our model seems able to reproduce important features of the phase diagram of expanded fullerides. In the following, we discuss the strongly correlated superconducting phase near the Mott transition, and also propose experiments that might distinguish it from a standard BCS state.

IV. UNDERSTANDING STRONGLY CORRELATED SUPERCONDUCTIVITY FROM DMFT AND THE IMPURITY MODEL

The reemergence of phonon-driven superconductivity close to the Mott transition [strongly correlated superconductivity (SCS)] was discussed by Capone *et al.* (2002) in terms of Fermi-liquid theory. A key point of that phenomenon is the renormalization of the effective bandwidth and thus of the effective mass, both controlled (in a Bethe lattice) by the quasiparticle weight Z, Eq. (13). $Z(U)$ decreases as a function of U/W and vanishes at the continuous metal-insulator transition point $U=U_c$, where the effective mass $m^*/m=1/Z(U)$ diverges and the effective quasiparticle bandwidth $W_*=ZW$ vanishes. An estimate of the interaction between charged quasiparticles requires the evolution of fluctuations that take place in charge space. Because charge fluctuations are gradually frozen away near the Mott transition, the effective repulsion between quasiparticles is also renormalized down to some smaller value $U_*<U$. In particular, the Fermi-liquid description provided by the Gutzwiller variational approach (Gutzwiller, 1963) and supported by the DMFT behavior of the average charge fluctuations $\langle(n-3)^2\rangle$, suggests that $U_*\simeq U\Gamma_U Z(U)^2 \sim UZ(U)$, where Γ_U includes all the so-called vertex corrections (Abrikosov *et al.*, 1965). This implies that the vertex function Γ_U diverges close to the Mott transition, but does not compensate the vanishing of Z (Capone *et al.*, 2002). The pairwise Jahn-Teller and exchange-based attraction J between quasiparticles, even if small, is restricted here to spin and orbital space, and has nothing to do with charge fluctuations. In other words, Hund's rule exchange and the JT coupling influence only the internal splitting of each molecular multiplet without affecting its center of gravity. As a result, this attraction should remain unrenormalized, $J_*=J\Gamma_J Z(U)^2\sim J$, close to the metal-insulator transition, thus implying a strongly divergent vertex correction Γ_J which cancels the vanishing Z. Therefore, the electron pair scattering amplitude A_* in the Cooper channel should renormalize as $A=U-\frac{10}{3}J\rightarrow A_*=Z(U)U-\frac{10}{3}J$. When U/W is small, $Z\lesssim 1$, the main effect of U is to suppress superconductivity, as noted earlier. However, if U is close to the critical metal-insulator value U_c, then $Z\sim(U_c-U)/U_c\ll 1$ and the scattering amplitude turns negative in spite of a large U. This is qualitatively the reason for the SCS reentrance of superconductivity [though in this region, of course, the actual pair scattering amplitude might deviate from this simple formula (Capone *et al.*, 2002)].

In addition, the Fermi-liquid argument suggests an explanation for the large value of the superconducting order parameter, implying a large T_c in the SCS regime (see Fig. 2) compared to the $U=0$ BCS values. In fact, when $A_*\simeq ZW$, and Z is dropping sharply, the quasiparticle attraction A_* will at some point ($U=U_*$) equal the coherent quasiparticle bandwidth ZW. That very uncommon situation of metallic quasiparticles with a pair attraction equal to their energy bandwidth is known to yield maximum superconductivity for a given attraction. As shown by studies of purely attractive models (Micnas *et al.*, 1990), the maximum superconducting temperature k_BT_c attainable in that case is about 7% of the pair attraction energy itself. In our model of trivalent fullerides, this estimate yields $k_BT_c\sim 0.07A_*\sim 0.2|J|$, which has the correct magnitude of roughly 40 K for $J\sim 20$ meV—a value in turn fully consistent with the observed spin gap 0.1 eV$\sim 5J$. While this coincidence of numbers is probably fortuitous, it does indicate that orders of magnitude implied by our model with realistic parameters are quite consistent with experimental facts. At face value, it also suggests that $0.07|J|=0.07(J_{\rm JT}-J_H)$ could be the maximum attainable k_BT_c in fullerides. We conclude that strong correlations play a crucial role in bringing the superconducting gap magnitude to the right range of values as compared with the experimental ones; see Fig. 4. Such values and large critical temperatures would never be attained within conventional BCS theory using $\lambda\simeq 0.16$–0.2, including as it should the large cancellation of JT interaction by exchange. They could in point of fact be attained if the cancellation due to exchange were (incorrectly) neglected, but then a lattice expansion should always lead to a decrease of T_c, contrary to experiment.

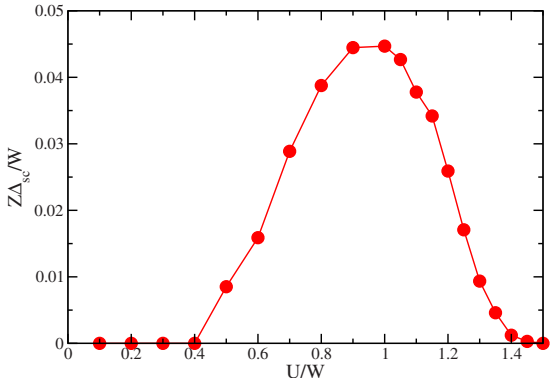

FIG. 4. (Color online) Quasiparticle superconducting energy gap in units of the bandwidth $W\simeq 0.6$ eV and on a larger scale than Fig. 3, computed through the anomalous self-energy [Fig. 2(a)] multiplied by the quasiparticle residue $Z(U)$. Note that, above $U/W\simeq 1.1$, the superconducting solution is metastable since the antiferromagnetic one has lower energy; see Fig. 2. We note that the maximum gap $Z\Delta_c\simeq 0.045W\simeq 27$ meV.

To appreciate further the effect of exchange-JT cancellation, it is instructive to consider [as was done for a simplified model by Capone *et al.* (2004)] the behavior with U/W of the superconducting self-energy $\Delta(0)$ (proportional to the $T=0$ gap, and roughly speaking to T_c) starting with pure JT and without exchange, and then proceeding to turn on exchange and gradual cancellation; see Fig. 5. For the bare JT interaction, $\lambda\simeq 1$ (a strong-coupling value), the superconducting self-energy decreases monotonically with increasing U, in agreement with the Migdal-Eliashberg prediction of an increasing Coulomb pseudopotential. Above a critical

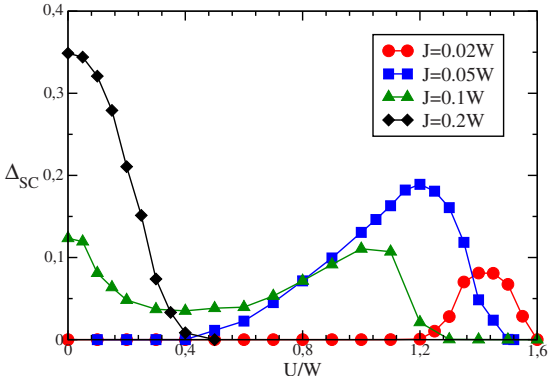

FIG. 5. (Color online) Anomalous self-energy $\Delta(0)$ (related to the superconducting gap by a factor Z^{-1}) for the superconducting solution and different values of the coupling parameter $J=0.02$, 0.05, 0.1, and 0.2, which correspond to $\lambda=0.09$, 0.21, 0.42, and 0.85, respectively. Note that for large J, corresponding to a case in which the Jahn-Teller coupling is not canceled by Hund's rule exchange, superconductivity is strongest at $U=0$. For increasing cancellation (decreasing J), two separate superconducting pockets emerge: a BCS pocket near $U=0$ and a SCS pocket near the Mott insulator. When the cancellation is nearly complete, the SCS pocket is many orders of magnitude stronger than the BCS. This is the situation we propose in our model of fullerides. Similar physics was described for a simpler model by Capone *et al.* (2004).

value, the system turns directly, via a second-order or weakly first-order phase transition, to a Mott insulating phase. This result is fully consistent with previous calculations by Han *et al.* (2003), where the same type of Hubbard model was studied within DMFT at finite temperature. Treating explicitly the electron-phonon coupling (including the full phonon dynamics) with $\lambda=0.6$ and neglecting exchange, they obtained a superconductor with monotonically decreasing gap.

Through a progressive reduction of λ (mimicking JT cancellation by exchange), we find that a nonmonotonic superconducting behavior makes its appearance as a function of U. Initially there is still a single superconducting phase for all U/W values, but two different regions near zero and near U_c begin to materialize. (Note that U_c simultaneously shifts to higher U as λ decreases.) When the cancellation is so strong that λ is still positive but small, the two superconducting regions break apart to form two separate pockets, leaving a normal-metal phase in between. In the leftmost pocket near $U/W=0$, the anomalous self-energy has a BCS-like exponential dependence on λ, and indeed superconductivity in this corner is of BCS type. Superconductivity in the rightmost pocket near the metal-insulator transition behaves quite differently. Here the λ dependence of superconductivity is much weaker, and the superconductive gap much stronger, than in the BCS pocket. Superconductivity in this pocket can in fact be characterized as SCS (Capone *et al.*, 2002), due to narrow quasiparticle pairing as described above. A similar behavior to Fig. 5, with two separate BCS and SCS regimes emerging from a single initial one when the effective pairing attraction is progressively weakened by exchange, was derived and illustrated in a simpler twofold-degenerate model by Capone *et al.* (2004).

The SCS superconducting pocket near the Mott transition is expected to differ from the BCS pocket even in its normal-state properties. The normal state underlying a BCS superconductor is Fermi-liquid-like. On the other hand, previous analyses suggest that the Fermi-liquid picture is likely to break down in our model when the Mott transition is approached. The key reason for the breakdown of the Fermi liquid is precisely that, when $Z\to 0$, the attraction between quasiparticles must eventually reach and exceed in magnitude the quasiparticle bandwidth ZW, a situation difficult to sustain.[3] Possible deviations from the Fermi-liquid paradigm were in fact overlooked by Capone *et al.* (2002) as they are related to the very-low-energy behavior of the normal phase close to the Mott transition, which was not explored in that work. Later, the non-Fermi-liquid behavior was discovered in the two-orbital model where the physics is very similar (Capone *et al.*, 2004).

A. Anderson impurity with a rigid bath

The DMFT calculations described above involved two steps, one solving the Anderson impurity model and the other making that self-consistent with the bath. Following reasoning proposed by Fabrizio *et al.* (2003), one may start off with the first step alone, namely, analyzing the bare AIM without imposing any self-consistency constraint. The conduction bath can be assumed to have a flat density of states, and the bath-impurity hybridization to be structureless, a situation that avoids numerical uncertainties and yields accurate low-energy properties. This kind of analysis applied to the AIM (3) shows (De Leo and Fabrizio, 2005) that two different impurity phases are stabilized according to the ratio between the attraction J and the Kondo temperature T_K (Hewson, 1997). Below this temperature and when $J=0$, the spin of an impurity coupled to a Fermi sea is screened out and absorbed in the conduction sea (Hewson, 1997). In the lattice context within DMFT, the Kondo scale measures metallic coherence and corresponds to the renormalized quasiparticle bandwidth ZW. For finite $J\neq 0$ but smaller than T_K, Kondo screening remains, thus still implying a Fermi-liquid behavior in DMFT. In fullerides, the impurity represents the C_{60}^{3-} ion, carrying three orbitals and three spins. In the Kondo phase, each of the three spins is separately screened by the bath and thus incorporated in the Fermi sea. Conversely, when $J>T_K$ the Kondo screening is lost, and that was shown to imply a non-

[3]Note that the high-energy Hubbard bands are unaffected by the small attraction J; superconductivity is just a matter of quasiparticles (Capone *et al.*, 2002). Therefore, a quasiparticle attraction exceeding their bandwidth cannot correspond to an instability toward a Mott insulator, which must involve also the Hubbard bands, but at most toward a breakdown of a quasiparticle-based Fermi liquid.

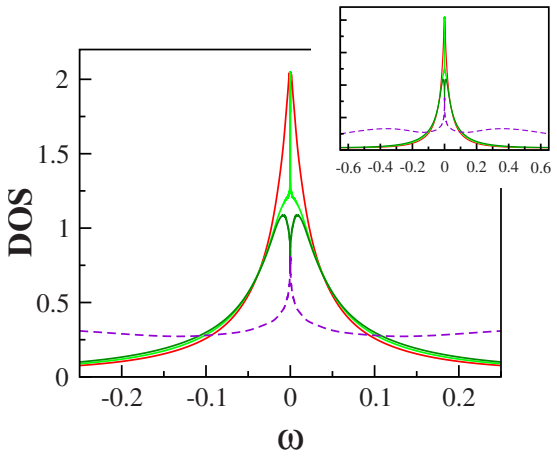

FIG. 6. (Color online) Impurity spectral function with a rigid bath characterized by a flat density of states (no DMFT self-consistency) across the critical point: the curves from top to bottom correspond to the evolution from the Kondo screened regime toward the pseudogap regime. The dotted line is the spectral function deep inside the non-Fermi-liquid phase $J \gg T_K$. Inset: The same curves plotted on a larger energy range, where the pseudogap of the dotted line is visible. The Fermi-liquid behavior corresponds to the normal state of the SCS superconducting phase for $J<J_{\rm cp}$ (analogous to the overdoped regime of cuprates), whereas the pseudogap behavior corresponds to the SCS normal state for $J>J_{\rm cp}$ (analogous to the underdoped cuprates). From De Leo and Fabrizio, 2005.

Fermi-liquid phase characterized by a pseudogap in the single-particle spectrum and by several other singular properties (De Leo and Fabrizio, 2005). A very qualitative description of this phase is that, unlike the Kondo phase, two spins out of three pair off antiferromagnetically at any given time, leaving out a single spin 1/2 available for Kondo screening. Since orbital degeneracy is unbroken, this residual spin $S=1/2$ also carries orbital momentum $L=1$, which corresponds to an overscreened non-Fermi-liquid situation (De Leo and Fabrizio, 2005). In this regime, it was predicted that the impurity contributions to the specific-heat coefficient and the pair susceptibility in the *s*-wave channel (14) diverge as $T^{-1/5}$ at low temperature T. In addition, the conduction electron scattering rate has a nonanalytic temperature behavior $T^{2/5}$. The local response functions to either a quadrupolar field, which splits the orbital degeneracy, or a magnetic field, which polarizes both spins and orbitals, also diverge as $T^{-1/5}$. The two phases, the Kondo screened phase and the pseudogap phase, are separated by a critical point at $J=J_{\rm cp}\simeq T_K$. It is endowed with a finite entropy $(1/2)\ln 3$, and with a divergent superconducting susceptibility with an exponent 1/3. As shown in Fig. 6, the single-particle spectral function displays strong deviations from a normal metal in the pseudogap phase and at the critical point.

Near this critical point, it has been found that the low-energy dynamics around the impurity is controlled by two separate energy scales (De Leo and Fabrizio, 2005), T_+ and T_-, whose behavior is very different as a function of increasing U/W. A higher energy scale T_+ is set by the critical $J_{\rm cp}\sim T_K$ and represents the width of a broad incoherent resonance; it evolves smoothly and uneventfully as the critical point is crossed (see Fig. 6). A lower energy scale $T_-\propto|J-T_K|^3$ measures instead the distance from the critical point, and leads simultaneously to a narrow resonance in the Fermi-liquid region and to an equally narrow spectral density dip (the "pseudogap") in the pseudogap phase (De Leo and Fabrizio, 2005). Since in this phase the impurity still carries a residual spin 1/2, there remains a finite value of the spectral function at the chemical potential, and the gap is not complete. The pseudogap widens if J is increased, and the cusplike dip in the impurity spectral function smoothly turns into a cusplike peak, the value at the chemical potential staying fixed and constant. This behavior is shown by the dotted curve in Fig. 6 corresponding to a very large pseudogap (see inset), possessing a very small peak at the chemical potential. This indicates the existence of yet another energy scale besides T_+ and T_- that sets the width of the cusp peak.

B. Anderson impurity with a self-consistent bath in DMFT

The rigid bath AIM behavior and its critical point reviewed above provide a guide to the DMFT results once the impurity-bath coupling is self-consistently determined. First, since T_K coincides within DMFT with the renormalized ZW, which in turn vanishes when the continuous Mott transition is approached, the impurity critical point is inevitably met before the metal-insulator transition as U/W is increased, at some $U_{\rm cp}\lesssim U_c$. This entails several important consequences:

- The normal state may be a Fermi liquid only far below the continuous metal-insulator transition, as may be the case in nonexpanded fullerides. Expanded compounds, on the other hand, are expected to have a non-Fermi-liquid normal state, and eventually a pseudogap, possibly developing before the first-order transition to the antiferromagnetic insulator.
- The SCS superconducting pocket near the Mott transition reflects the leading instability of the impurity critical point. In other words, SCS superconductivity is the way in which the lattice model responds to impurity criticality and avoids it.
- The lower-energy scale vanishes right at the critical point, $T_-=0$. Here $T_+\simeq J$ thus remains as the only energy scale controlling the magnitude of the superconducting energy gap. Away from $U=U_{\rm cp}$, $T_-\neq 0$, and the amplitude of the superconducting gap should decrease monotonically with increasing $(T_+-T_-)/T_+$ (Capone *et al.*, 2004) since T_- cuts offs the local pairing instability. Therefore, the gap should be maximum right at the impurity critical point (the top of the dome).
- Even though the normal phase is non-Fermi-liquid, well-defined Bogoliubov quasiparticles should exist

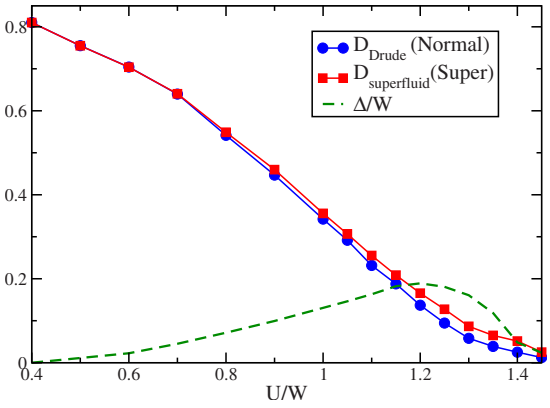

FIG. 7. (Color online) Calculated weights of the zero-frequency delta-function contribution to the optical conductivity for the superconducting phase (superfluid stiffness, squares) and the normal phase (Drude weight, circles). The zero-frequency anomalous self-energy is also plotted. Note the higher values in the SCS superconductor relative to the non-superconducting metal phase.

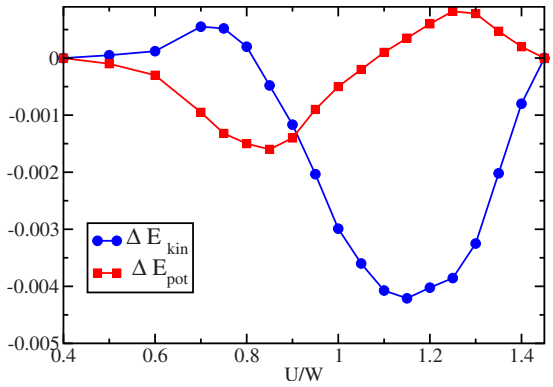

FIG. 8. (Color online) Energetic balance underlying superconductivity. $\Delta E_{\rm pot}=E^S_{\rm pot}-E^N_{\rm pot}$ is the difference between the potential energies of the superconducting and normal solutions, while $\Delta E_{\rm kin}=E^S_{\rm kin}-E^N_{\rm kin}$ is the same difference between the kinetic energies of the two solutions.

inside the SCS superconducting pocket.

The last statement comes from the fact that, at the impurity critical point, superconductivity provides a new screening channel that helps the system get rid of the finite residual entropy at the critical point, thus eliminating non-Fermi-liquid singularities (De Leo and Fabrizio, 2005; Schirò *et al.*, 2008).

The role of superconductivity as a novel screening channel close to the impurity model critical point should be reflected, in the lattice model, into a gain of band energy (the tight-binding "kinetic energy") at the onset of superconductivity. Owing to a sum rule connecting kinetic energy and zero-frequency optical conductivity (sometimes referred to as the Drude weight) (Scalapino *et al.*, 1993), the onset of SCS superconductivity close to the Mott transition should lead to a Drude weight increase. This prediction is borne out by the full DMFT solution of our Hamiltonian. In Fig. 7, we plot the $\omega=0$ (dc) optical conductivity of our model superconductor (where it coincides with the superfluid stiffness), defined by (Toschi *et al.*, 2005)

$$D_s = -E_{\rm kin} + \chi_{jj}(\mathbf{q}\to\mathbf{0},\Omega=0), \tag{16}$$

where $E_{\rm kin}$ is the kinetic energy and χ_{jj} is the static limit of the paramagnetic part of the electromagnetic kernel,

$$\chi_{jj} = \frac{2}{\beta}\sum_n \int d\epsilon\, N(\epsilon)V(\epsilon)[G(\epsilon,\omega_n)G^*(\epsilon,\omega_n) + F(\epsilon,\omega_n)F(\epsilon,\omega_n)], \tag{17}$$

where $V(\epsilon)=(4t^2-\epsilon^2)/3$ is the current vertex in the Bethe lattice while $G(\epsilon,\omega_n)$ and $F(\epsilon,\omega_n)$ are the normal and anomalous lattice Green's functions, respectively. In the same figure, we also plot the zero-frequency dc conductivity (the Drude weight) of the underlying metastable solution where superconductivity is inhibited; this state is meant to provide a sketch of the real normal phase above T_c. The Drude weight is given by Eqs. (16) and (17) with $F(\epsilon,\omega_n)\equiv 0$. Upon entering the SCS dome from the low-U/W side, the superconducting phase initially loses kinetic energy compared to the normal state as in ordinary BCS theory. However, as U/W increases to and beyond the dome maximum, the loss changes to a gain, and indeed most of the SCS superconducting pocket is predicted to have a larger weight of the zero-frequency optical absorption than the nonsuperconducting state. The same behavior is displayed (Fig. 8) by the energy balance between the two solutions. Only far below the Mott transition is the superconductor stabilized by a potential energy gain, as is the case in BCS theory. In the pseudogap regime, corresponding to the expanded fullerides near the Mott transition, the stabilization is associated with a kinetic energy gain.

A similar phenomenon is well known in the optical conductivity of high-T_c copper oxides (Carbone *et al.*, 2006). Our calculations show that an increase in the zero-frequency optical conductivity or a kinetic energy gain does not actually exclude an electron-phonon pairing mechanism, but rather demonstrates the key importance of strong electronic correlations. Thanks to pairing, the motion of carriers in the superconducting phase is facilitated with respect to the pseudogap nonsuperconducting metal. In that anomalous metal (a non-Fermi-liquid) the interaction constraints jam the free propagation of quasiparticles, causing a kinetic energy cost, partly released with the onset of superconductivity. It would be of interest if the optical conductivity increase demonstrated in cuprates could be investigated in fullerides, both regular and expanded, since that would help discriminate between conventional BCS superconductivity and SCS.

V. DISCUSSION OF EXPERIMENTAL PROBES

In the following, we discuss whether and how the dominance of strong correlation we propose for the superconducting fullerides can be reconciled with the list

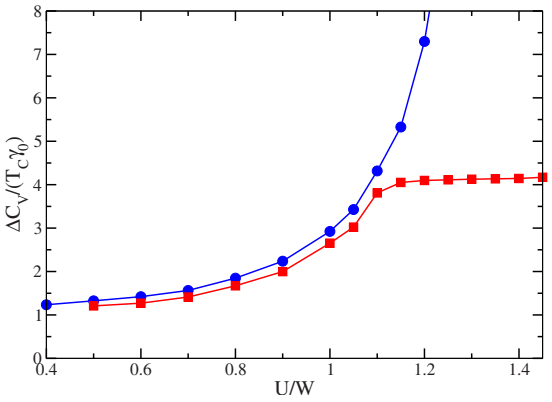

FIG. 9. (Color online) Specific-heat jump, in units of $T_c\gamma_0$, as a function of U/W. For comparison we also show the behavior of $1/Z(U)$, which should correspond to the same quantity if Fermi-liquid theory is valid.

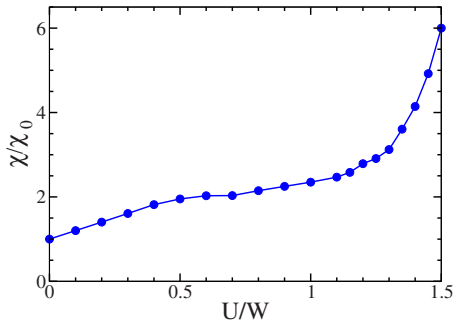

FIG. 10. (Color online) Normal-phase uniform magnetic susceptibility χ normalized to the noninteracting value χ_0. For $U=0$, $\chi\simeq\chi_0$, the difference being extremely small since $J\ll W$. The plateau between $U/W=0.5$ and 1 signals the effective crossover from a Fermi liquid with $S=3/2$ per site to a non-Fermi-liquid with $S=1/2$ per site.

of experimental facts given earlier, supporting a conventional BCS behavior. The first quantity we discuss is the specific-heat jump at T_c. Within BCS theory, the specific-heat jump ΔC_V at T_c is

$$\Delta C_V/T_c \simeq 1.52\gamma_*, \tag{18}$$

where γ_* is the specific-heat coefficient of the metallic phase ($C_V=\gamma_* T$), proportional to the mass enhancement m^*/m, in our case $1/Z$. The measured specific-heat jump leads, through Eq. (18), to an estimate of $\gamma_*\simeq 3\gamma_0$. This is indeed a rather low and regular value that has been commonly advocated as evidence of weak correlations in fullerenes. However, the standard argument holds only if the normal phase is of Fermi-liquid type, which is not applicable close to a Mott transition, independent of any model.

In Fig. 9 we plot the jump in C_V at T_c for increasing U/W, compared with the Fermi-liquid estimate $1/Z$.[4] After a region where the calculated quantity closely follows $1/Z$, $\Delta C_V/T_c$ flattens out and stays roughly constant around $4\gamma_0$ up to the Mott transition, despite a diverging $1/Z$ (see Fig. 9). This shows that the energy scale that controls the superconducting instability is constant near the Mott transition, consistent with the single-impurity prediction that this scale should be identified by T_+, a quantity of order J. The conclusion here is that a normally sized specific-heat jump does not imply BCS superconductivity in fullerides.

Another physical quantity that seemingly pointed toward weak correlations in fullerides is the magnetic susceptibility measured in the normal phase, consistent with a weakly correlated Fermi liquid and a Stoner enhancement of about a factor 2–3. This argument again becomes inconclusive once the Fermi-liquid scenario is abandoned. In Fig. 10 we plot as a function of U/W the uniform magnetic susceptibility in the normal phase calculated by DMFT. After an initial Stoner enhancement at small U/W, the susceptibility flattens out and remains almost constant before a rapid growth, which takes place close to the Mott transition. In the plateau region, the susceptibility enhancement is a factor between 2 and 3 with respect to the value at $U=0$, surprisingly close to the experimental enhancement, covering the whole superconducting domain. Physically, the origin of this susceptibility plateau for increasing U is quite instructive. It corresponds to the gradual crossover of the maximum spin available at each site from $S=3/2$ in the Fermi liquid at small $U<U_{cp}$ (Kondo screened AIM) to $S=1/2$ near Mott and large $U>U_{cp}$, where Fermi-liquid behavior is lost. In essence, at large U, each molecule is effectively in a (dynamically) JT-distorted state, where two out of three electrons are spin paired (Auerbach *et al.*, 1994). We are thus led to conclude that the relatively weak observed enhancement of susceptibility does not correspond to a Stoner-enhanced, weakly correlated Fermi liquid—in fact, quasiparticles do not even exist in most of the plateau region.

Finally, we address signatures of the strongly correlated scenario that we expect will show up in spectroscopies including the tunneling I-V characteristics and angle-resolved photoemission spectroscopy (ARPES). This is initially embarrassing on two accounts. First, ARPES spectroscopies are **k**-vector resolved, whereas in DMFT we do not have access to any spatial structure. Second, tunneling spectroscopies are extremely well resolved near zero voltage, whereas our Lanczos method yields a much poorer spectral function resolution in this region.

We address tunneling first. Although Fig. 6 refers to the impurity C_{60}^{3-} molecule, we believe that similar features would remain after imposing full DMFT self-consistency in the normal phase—if we had a better low-

[4]As mentioned in Sec. III.A, for the present three-orbital model it has not been practical to include in Eq. (6) a number of excited states sufficient to make the truncation error in the Green's function negligible. For the data reported in Fig. 9 we have an average error of 3–4 %, which does not allow us to determine T_c with sufficient accuracy. Yet the jump of the specific heat relative to T_c turns out to be almost independent of the truncation error and the details of the calculations.

frequency numerical resolution than we presently have. Hence, we suggest that tunneling I-V spectra of expanded fullerides be measured and examined, in order to bring out the expected rich structure of the type sketched in Fig. 6.

Next, we consider photoelectron spectroscopy. Again, according to the single-impurity analysis (De Leo and Fabrizio, 2005), the imaginary part of the single-particle self-energy should be finite and of order T_+ almost everywhere in the non-Fermi-liquid normal phase above T_c. This has the following implications for ARPES:

- The fulleride photoemission spectrum should show t_{1u} bands dispersing in the Brillouin zone with nonzero bandwidth, governed by the energy scale T_+. The value of T_+ decreases with increasing U/W (increasing expansion), from W at $U=0$ to (larger than) J at the Mott transition.
- There should be a spectral peak broadening of the same order of magnitude T_+ as the apparent **k**-resolved band dispersion. In particular, the broadening should remain constant on approaching the Fermi surface—unlike a Fermi-liquid phase where quasi-particle peaks become narrower and narrower.

The momentum independence of the DMFT self-energy implies that, in this approximation, the **k** modulation of the electronic dispersion is assumed to remain unaffected by interactions. Within this assumption and without requiring too high accuracy in frequency, we can compute a toy **k**-resolved spectral function according to

$$A(k,\omega) = -\frac{1}{\pi}\,\mathrm{Im}\,\frac{1}{\omega - \varepsilon_{\mathbf{k}} - \Sigma_{\mathrm{DMFT}}(\omega)}, \tag{19}$$

where $\varepsilon_{\mathbf{k}}$ is the noninteracting dispersion and $\Sigma_{\mathrm{DMFT}}(\omega)$ is the DMFT self-energy calculated with a finite number of baths. The effect of the local self-energy will be to change the effective bandwidth and give rise to finite-lifetime effects, even if the **k** modulation of the dispersion is unrenormalized. For our Bethe lattice, there is no straightforward definition of momentum, and we remedy that by computing $A(\varepsilon,\omega)$, which corresponds to Eq. (19) with $\varepsilon_{\mathbf{k}} \to \varepsilon$.

In Fig. 11 we show theoretical ARPES results for some choices of ε obtained using the DMFT self-energy for temperatures above T_c, both for a value of $U/W=1.1$, which lies close to the maximum of the superconducting dome but still on the less correlated side, corresponding to unexpanded (or moderately expanded) fullerides, and for a value that lies in the downward branch of the dome ($U/W=1.3$), corresponding to a highly expanded fulleride. We note in both cases the existence of an incoherent low-energy feature dispersing with a reduced but nonzero electron bandwidth of $0.1W$. In the expanded case, the pseudogap feature is clearly present.

Recent photoemission spectra of K_3C_{60} (Goldoni, 2007) indicate an overall dispersion bandwidth of about 160 meV, about a quarter of the bare calculated bandwidth in the local-density approximation. The experimental spectral peak does not show the usual Fermi-liquid-like narrowing on approaching the Fermi level, a fact that is in agreement with our expectation for a non-Fermi-liquid (although a nonexpanded fulleride like K_3C_{60} probably lies at the beginning of the SCS dome, where deviations from Fermi-liquid behavior are not large). Experimentally the peak does not appear to cross the Fermi level, and the intensity instead drops, suggestive of a pseudogap. Unfortunately, the spectrum shows very strong vibronic effects, reflecting the retarded strong electron Jahn-Teller coupling. This aspect is not covered by our unretarded approximation, but it heavily affects the line shape and hampers the extraction of purely electronic features. Treatment of the vibronic effects, and a quantitative description of dispersion, will require abandoning in the future our approximation of infinitely fast phonon dynamics, as well as a possible extension to cluster extensions of DMFT that allow for different renormalizations of different momenta (Hettler *et al.*, 2000; Kotliar *et al.*, 2001).

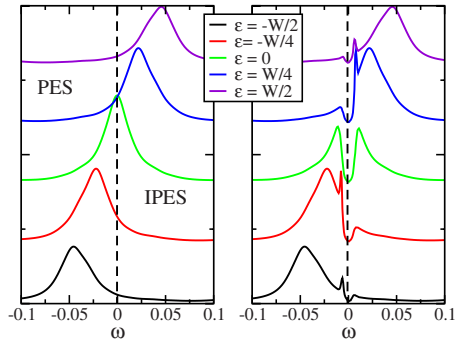

FIG. 11. (Color online) Simulated photoemission spectra elaborated from the DMFT result in the normal phase. The left panel refers to $U/W=1.1$ (corresponding to unexpanded fullerides), while the right panel is for $U/W=1.3$ (corresponding to expanded fullerides).

VI. CONCLUSIONS

Summarizing, we addressed the contradictory properties of expanded trivalent fulleride superconductors and insulators—and to some extent of the whole family of fullerides—and presented a theoretical scenario emphasizing the role of strong electron correlations. The scenario is especially designed and appropriate for the more expanded members of the family, such as $(NH_3)_xNaK_2C_{60}$, Li_3C_{60}, $Cs_{3-x}K_xC_{60}$, and $Cs_{3-x}Rb_xC_{60}$, and the recently discovered $A15$ Cs_3C_{60}, which are near or past the Mott transition.

Our model explains the dome-shaped increase and subsequent decrease of T_c upon expansion of the lattice spacing in fullerides, the coexistence of metallic behavior and of Mott insulator features such as the large NMR spin gap in all fullerides, and the $S=1/2$ spin in the insulating state (identified as a Mott-Jahn-Teller insulator). It explains why the s-wave T_c can be as high as 40 K even though the Coulomb interaction strength is prohibitive, and why T_c does not automatically decrease

upon increase of U/W. It also accounts for more standard observations, such as regular specific-heat jumps and moderately high spin susceptibilities, facts that were previously construed as evidence for conventional BCS superconductivity.

In addition to those listed in the previous section, one can anticipate a number of additional experiments that could provide incontrovertible evidence for strongly correlated superconductivity in fullerides. The tunneling I-V characteristics observable, e.g., by a scanning tunneling spectroscopy tip, should, in an expanded fulleride, develop the low-energy features typical of the Kondo impurity spectral function. The isotope effect upon carbon substitution should also behave very unconventionally, and eventually get smaller as the superconducting dome is passed and the Mott transition is approached upon expansion. In this regime, as the quasiparticle bandwidth ZW gradually falls below the typical energy $\hbar\omega$ of an increasing fraction of the eight H_g Jahn-Teller modes, the associated retardation effect should in fact disappear. The expanded fullerides and related materials, clearly not investigated sufficiently so far, deserve in our view the highest experimental attention. They combine elements that make them members of an expanded high-temperature superconductor family. They combine the neighborhood of the Mott transition and the predominance of strong electron correlations with conventional elements such as electron-phonon s-wave pairing, which are typical of BCS systems. Our study identifies a pseudogap and other features in the I-V tunneling spectrum, an increase of zero-frequency optical weight in the optical response of the superconducting phase, and the emergence of two separate energy scales in ARPES as the most urgent experimental undertakings that could confirm or falsify our claims.

ACKNOWLEDGMENTS

E.T. thanks Kosmas Prassides, Andrea Goldoni, and Mauro Ricco' for information and discussion about fullerides, and Kosmas Prassides for providing Fig. 1. M.C. acknowledges discussions with A. Toschi. Work in SISSA was sponsored by PRIN Cofin 2006022847, as well as by INFM/CNR "Iniziativa trasversale calcolo parallelo." Work in Rome was sponsored by PRIN Cofin 200522492.

REFERENCES

Abrikosov, A. A., L. P. Gor'kov, and I. E. Dzyaloshinskii, 1965, *Quantum Field Theoretical Methods in Statistical Physics* (Pergamon, Oxford).
Anderson, P. W., 1987, Science **235**, 1196.
Auerbach, A., N. Manini, and E. Tosatti, 1994, Phys. Rev. B **49**, 12998.
Bardeen, J., L. N. Cooper, and J. R. Schrieffer, 1957a, Phys. Rev. **106**, 162.
Bardeen, J., L. N. Cooper, and J. R. Schrieffer, 1957b, Phys. Rev. **108**, 1175.
Baskaran, G., and E. Tosatti, 1991, Curr. Sci. **61**, 33.
Bennemann, K. H., and J. B. Ketterson, 2008, Eds., *Superconductivity* (Springer, Berlin).
Brouet, V., H. Alloul, S. Garaj, and L. Forró, 2002a, Phys. Rev. B **66**, 155122.
Brouet, V., H. Alloul, S. Garaj, and L. Forró, 2002b, Phys. Rev. B **66**, 155124.
Burkhart, G. J., and C. Meingast, 1996, Phys. Rev. B **54**, R6865.
Capone, M., L. de' Medici, and A. Georges, 2007, Phys. Rev. B **76**, 245116.
Capone, M., M. Fabrizio, C. Castellani, and E. Tosatti, 2002, Science **296**, 2364.
Capone, M., M. Fabrizio, C. Castellani, and E. Tosatti, 2004, Phys. Rev. Lett. **93**, 047001.
Capone, M., M. Fabrizio, P. Giannozzi, and E. Tosatti, 2000, Phys. Rev. B **62**, 7619.
Capone, M., M. Fabrizio, and E. Tosatti, 2001, Phys. Rev. Lett. **86**, 5361.
Cappelluti, E., C. Grimaldi, L. Pietronero, and S. Strässler, 2000, Phys. Rev. Lett. **85**, 4771.
Carbone, F., A. B. Kuzmenko, H. J. A. Molegraaf, E. van Heumen, E. Giannini, and D. van der Marel, 2006, Phys. Rev. B **74**, 024502, and references therein.
Chakravarty, S., M. Gelfand, and S. Kivelson, 1991, Science **254**, 970.
Chakravarty, S., and S. Kivelson, 2001, Phys. Rev. B **64**, 064511.
Dahlke, P., M. S. Denning, P. F. Henry, and M. J. Rosseinsky, 2000, J. Am. Chem. Soc. **122**, 12352.
Dahlke, P., and M. J. Rosseinsky, 2002, Chem. Mater. **14**, 1285.
De Leo, L., and M. Fabrizio, 2005, Phys. Rev. Lett. **94**, 236401.
Durand, P., G. R. Darling, Y. Dubitsky, A. Zaopo, and M. J. Rosseinsky, 2003, Nature Mater. **2**, 605.
Eliashberg, G. M., 1960a, Zh. Eksp. Teor. Fiz. **38**, 966 [Sov. Phys. JETP **11**, 696 (1960)].
Eliashberg, G. M., 1960b, Zh. Eksp. Teor. Fiz. **39**, 1437 [Sov. Phys. JETP **12**, 1000 (1960)].
Erwin, S. C., 1993, in *Buckminsterfullerenes*, edited by W. Billups and M. Ciufolini (VHC, New York), p. 217.
Fabrizio, M., A. F. Ho, L. De Leo, and G. E. Santoro, 2003, Phys. Rev. Lett. **91**, 246402.
Fabrizio, M., and E. Tosatti, 1997, Phys. Rev. B **55**, 13465.
Ganin, A. Y., Y. Takabashi, Y. Z. Khimyak, S. Margadonna, A. Tamai, M. J. Rosseinsky, and K. Prassides, 2008, Nature Mater. **7**, 367.
Georges, A., G. Kotliar, W. Krauth, and M. J. Rozenberg, 1996, Rev. Mod. Phys. **68**, 13.
Goldoni, A., 2007, unpublished.
Granath, M., and S. Östlund, 2003, Phys. Rev. B **68**, 205107.
Gunnarsson, O., 1997, Rev. Mod. Phys. **69**, 575.
Gunnarsson, O., 2004, *Alkali-Doped Fullerides: Narrow-Band Solids with Unusual Properties* (World Scientific, Singapore).
Gunnarsson, O., H. Handschuh, P. S. Bechthold, B. Kessler, G. Ganterör, and W. Eberhardt, 1995, Phys. Rev. Lett. **74**, 1875.
Gutzwiller, M. C., 1963, Phys. Rev. Lett. **10**, 159.
Han, J. E., O. Gunnarsson, and V. H. Crespi, 2003, Phys. Rev. Lett. **90**, 167006.
Hettler, M. H., M. Mukherjee, M. Jarrell, and H. R. Krishnamurthy, 2000, Phys. Rev. B **61**, 12739.
Hewson, A., 1997, *The Kondo Problem to Heavy Fermions* (Cambridge University Press, Cambridge, UK).
Huq, A., and P. W. Stephens, 2006, Phys. Rev. B **74**, 075424.
Iwasa, Y., and T. Takenobu, 2003, J. Phys.: Condens. Matter **15**,

R495, and references therein.
Kitano, H., R. Matsuo, K. Miwa, A. Maeda, T. Takenobu, Y. Iwasa, and T. Mitani, 2002, Phys. Rev. Lett. **88**, 096401.
Klupp, G., K. Kamarás, N. M. Nemes, C. M. Brown, and J. Leão, 2006, Phys. Rev. B **73**, 085415.
Knupfer, M., and J. Fink, 1997, Phys. Rev. Lett. **79**, 2714.
Kotliar, G., S. Y. Savrasov, G. Palsson, and G. Biroli, 2001, Phys. Rev. Lett. **87**, 186401.
Landau, L. D., and E. M. Lifshitz, 1958, *Quantum Mechanics: Non-Relativistic Theory* (Pergamon, New York).
Lannoo, M., G. Baraff, M. Schluter, and D. Tomanek, 1991, Phys. Rev. B **44**, 12106.
Lof, R., M. van Veenendaal, B. Koopmans, H. Jonkman, and G. Sawatzky, 1992, Phys. Rev. Lett. **68**, 3924.
Lüders, M., A. Bordoni, N. Manini, A. Dal Corso, M. Fabrizio, and E. Tosatti, 2002, Philos. Mag. B **82**, 1611.
Martin, R. L., and J. P. Ritchie, 1993, Phys. Rev. B **48**, 4845.
Micnas, R., J. Ranninger, and S. Robaszkiewicz, 1990, Rev. Mod. Phys. **62**, 113.
Migdal, A. B., 1958, Zh. Eksp. Teor. Fiz. **34**, 1438 [Sov. Phys. JETP **7**, 996 (1958)].
Mott, N. F., 1990, *Metal Insulator Transition* (Taylor and Francis, London).
Onnes, H. K., 1911, Commun. Phys. Lab. Univ. Leiden **120b, 122b, 124c**.
Palstra, T. T. M., O. Zhou, Y. Iwasa, P. E. Sulewski, R. M. Fleming, and B. R. Zegarski, 1995, Solid State Commun. **93**, 327.
Parks, R. D., 1969, Ed., *Superconductivity* (Dekker, New York).
Prassides, K., S. Margadonna, D. Arcon, A. Lappas, H. Shimoda, and Y. Iwasa, 1999, J. Am. Chem. Soc. **121**, 11227.
Ramirez, A. P., 1994, Supercond. Rev. **1**, 1.
Ramirez, A. P., A. R. Kortan, M. J. Rosseinsky, S. J. Duclos, A. M. Mujsce, R. C. Haddon, D. W. Murphy, A. V. Makhija, S. M. Zahurak, and K. B. Lyons, 1992, Phys. Rev. Lett. **68**, 1058.
Riccó, M., G. Fumera, T. Shiroka, O. Ligabue, C. Bucci, and F. Bolzoni, 2003, Phys. Rev. B **68**, 035102.
Robert, J., P. Petit, T. Yildirim, and J. E. Fischer, 1998, Phys. Rev. B **57**, 1226.
Satpathy, S., V. P. Antropov, O. K. Andersen, O. Jepsen, O. Gunnarsson, and A. I. Liechtenstein, 1992, Phys. Rev. B **46**, 1773.
Scalapino, D. J., S. R. White, and S. Zhang, 1993, Phys. Rev. B **47**, 7995.
Schirò, M., M. Capone, M. Fabrizio, and C. Castellani, 2008, Phys. Rev. B **77**, 104522.
Thier, K.-F., G. Zimmer, M. Mehring, and F. Rachdi, 1995, in *Physics and Chemistry of Fullerenes and Derivatives*, edited by H. Kuzmany, O. Fink, M. Mehring, and S. Roth (World Scientific, Singapore), p. 432.
Toschi, A., M. Capone, and C. Castellani, 2005, Phys. Rev. B **72**, 235118.
Varma, C., J. Zaanen, and K. Raghavachari, 1991, Science **254**, 989.
Wachowiak, A., R. Yamachika, K. H. Khoo, Y. Wang, M. Grobis, D.-H. Lee, S. G. Louie, and M. F. Crommie, 2005, Science **310**, 468.
Yildirim, Y., J. E. Fisher, R. Dinnebier, P. W. Stephens, and C. L. Lin, 1995, Solid State Commun. **93**, 295.
Zhou, O., T. T. M. Palstra, Y. Iwasa, R. M. Fleming, A. F. Hebard, and P. E. Sulewski, 1995, Phys. Rev. B **52**, 483.